Original Article

Validation of the commercial coronary computed tomographic angiography artificial intelligence for coronary artery stenosis: a cross-sectional study

Qi Han[1#], Feihua Jing[2#], Zhiguo Sun[3], Fei Liu[4], Jucai Zhang[5], Jian Wang[1], Hongqin Liang[1^]

[1]Department of Radiology, Southwest Hospital, Third Military Medical University (Army Medical University), Chongqing, China; [2]Department of Radiology, Linfen Central Hospital, Linfen, China; [3]Department of Interventional Radiology, UIanqab Central Hospital, UIanqab, China; [4]Department of Radiology, Nanjing Medical University Second Affiliated Hospital, Nanjing, China; [5]Department of Radiology, The Second People Hospital of Liaocheng, Liaocheng, China

Contributions: (I) Conception and design: Q Han, H Liang; (II) Administrative support: J Wang; (III) Provision of study materials or patients: Q Han, F Jing, Z Sun, J Zhang; (IV) Collection and assembly of data: Q Han, F Jing, F Liu; (V) Data analysis and interpretation: Q Han, F Jing, J Wang, H Liang; (VI) Manuscript writing: All authors; (VII) Final approval of manuscript: All authors.

[#]These authors contributed equally to this work and should be considered as co-first authors.

Correspondence to: Jian Wang. Department of Radiology, Southwest Hospital, Third Military Medical University (Army Medical University), 30 Gaotanyan Road, Shapingba District, Chongqing 400038, China. Email: 649672652@qq.com; Hongqin Liang. Department of Radiology, Southwest Hospital, Third Military Medical University (Army Medical University), 30 Gaotanyan Road, Shapingba District, Chongqing 400038, China. Email: 46778207@qq.com.

Background: The commercial coronary computed tomographic angiography artificial intelligence (CCTA-AI) platform has made great progress in clinical application. However, research is needed to elucidate the current stage of commercial AI platforms and the role of radiologists. This study compared the diagnostic performance of the commercial CCTA-AI platform with that of a reader based on a multicenter and multidevice sample.

Methods: A total of 318 patients with suspected coronary artery disease (CAD) who underwent both CCTA and invasive coronary angiography (ICA) were included in a multicenter and multidevice validation cohort between 2017 and 2021. The commercial CCTA-AI platform was used to automatically assess coronary artery stenosis by using ICA findings as the gold standard. The CCTA reader was completed by radiologists. The diagnostic performance of the commercial CCTA-AI platform and CCTA reader was evaluated at the patient and segment levels. The cutoff values of models 1 and 2 were 50% and 70% stenosis, respectively.

Results: It took 20.4 seconds to accomplish post-processing per patient when using the CCTA-AI platform, which was significantly shorter than the time taken to complete this task with the CCTA reader (1,112.1 s). In the patient-based analysis, the area under the curve (AUC) was 0.85 using the CCTA-AI platform and 0.61 using the CCTA reader in model 1 (stenosis ratio: 50%). In contrast, the AUC was 0.78 using the CCTA-AI platform and 0.64 using the CCTA reader in model 2 (stenosis ratio: 70%). In the segment-based analysis, the AUCs of CCTA-AI were slightly better than those of the readers. The negative predictive value (NPV) increased from model 1 to model 2. Furthermore, the diagnostic performance was better for larger-diameter arteries.

Conclusions: The commercial CCTA-AI platform may provide a feasible solution for the diagnosis of coronary artery stenosis, and it has a diagnostic performance that is slightly better than that of a radiologist with a moderate level of experience (5–10 years of experience).

^ ORCID: 0000-0002-0880-6186.

Keywords: Coronary artery computed tomographic angiography; coronary artery disease (CAD); coronary artery stenosis; artificial intelligence (AI)

Submitted Oct 14, 2022. Accepted for publication Mar 22, 2023. Published online Apr 12, 2023.
doi: 10.21037/qims-22-1115
View this article at: https://dx.doi.org/10.21037/qims-22-1115

Introduction

Coronary artery disease (CAD), also known as coronary atherosclerosis, results in myocardial ischemia and necrosis (1). CAD is currently one of the leading causes of death worldwide (2). Despite the development of drugs and interventional therapies, the clinical prognoses of patients with CAD are still poor. Accurate assessment and management of the risk factors for CAD are very important for optimal treatment selection and the prognosis of patients (3). Although invasive coronary angiography (ICA) is the gold standard for assessing the severity of CAD, it is an invasive examination associated with high medical costs (4).

Coronary computed tomographic angiography (CCTA) is the first-line investigation for suspected chest pain (5). CCTA can clearly show the structure of the heart and coronary artery. A radiologist can use this to assess the degree of coronary artery stenosis and the characteristics of the plaque and classify the patient's risk (6). CCTA provides a useful noninvasive imaging method for the initial diagnosis of CAD (7,8). However, the diagnosis of CAD using CCTA requires manual image post-processing and subjective visual observation by the radiologist, which demands significant human resources and time and lacks efficiency and accuracy (9).

Artificial intelligence (AI) has rapidly gained popularity over recent years, and the application of AI in the medical field has become commonplace (10). In the cardiovascular field, AI technology could significantly speed up cardiovascular image reconstruction, provide an objective means of image segmentation, and be used to evaluate the degree of vascular stenosis (11,12). AI technology can also be used to assess calcification and the computed tomography fractional flow reserve (CT-FFR) (13). Recent research has focused on the reconstruction and optimization of AI models based on machine learning, including supervised learning, unsupervised learning, and deep learning (DL), which is the main technology of AI. Supervised learning includes many techniques and algorithms, such as artificial neural networks, support vector machines, decision trees, and random forests (14,15). DL includes convolutional neural networks (CNNs), recurrent neural networks, and deep neural networks (16,17). AI technology differs in its applications and limitations for different data types. Therefore, finding an appropriate intelligent mathematical model could facilitate accurate diagnosis of CAD. Some studies have started to address the diagnostic efficiency of AI for CAD and verified the feasibility of this based on CCTA using DL (18,19). There exist a few commercial coronary computed tomographic angiography artificial intelligence (CCTA-AI) platforms that can be used in the cardiovascular clinic for image post-processing and diagnosis. However, there is not enough research that tests the CCTA-AI platforms' actual levels of diagnostic performance at the segment and lesion levels based on multicenter and multidevice data.

We hypothesized that AI-based assisted analysis is at a level equivalent to that of expert readers with 5–10 years of experience in assessing coronary artery morphology and stenosis. Using ICA as the gold standard, this study compared CCTA-AI with radiological readers to identify the current stage of commercial AI platforms and the role of radiologists by completely external data from different CT models in multicenter hospitals. In addition, this study further verified the generalization ability of contemporary commercial algorithm models. We present the following article in accordance with the STARD reporting checklist (available at https://qims.amegroups.com/article/view/10.21037/qims-22-1115/rc).

Methods

Patient population

The study was conducted in accordance with the Declaration of Helsinki (as revised in 2013). This study was approved by Southwest Hospital, Third Military Medical University [Army Medical University (No. KY2020306)] and the medical science research ethics committees of 3 other hospitals [The Second People's Hospital of Liao Cheng (No. 2021-8); UIanqab Central Hospital (No. 2021-3);

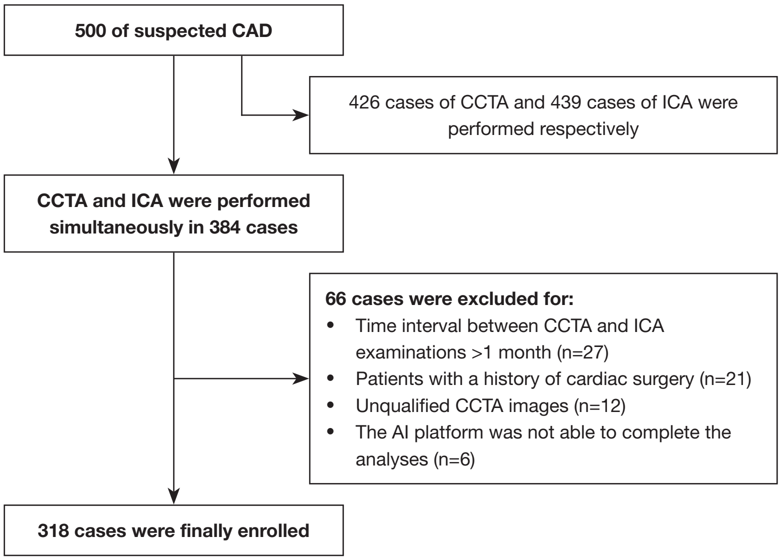

Figure 1 The flow diagram shows the study inclusion and exclusion criteria. CAD, coronary artery disease; CCTA, coronary computed tomographic angiography; ICA, invasive coronary angiography; AI, artificial intelligence.

LinFen central hospital (ethics approval No. 2021-23-1)]. The requirement for individual consent for this retrospective analysis was waived. This retrospective study involved 4 general hospitals in western [Southwest Hospital, Third Military Medical University (Army Medical University)], eastern (The Second People's Hospital of Liao Cheng), northeast (UIanqab Central Hospital), and central (LinFen central hospital) China. Patients with suspected chest pain who underwent CCTA and ICA in these hospitals between January 2017 and December 2021 were retrospectively reviewed.

All patients subsequently underwent ICA within 1 month of their CCTA scan. The exclusion criteria were as follows: (I) patients with a history of cardiac surgery, including coronary artery bypass grafting or percutaneous coronary intervention; (II) patients for whom the AI platform was not able to complete the analyses; (III) patients for whom the diagnostic image quality of CCTA or ICA did not meet the requirement [classified as either poor or sufficient (20)]. The flowchart of this study is displayed in *Figure 1*.

Image acquisition

Patients were scanned on either a second-generation dual-source CT system (SOMATOM Definition Flash, Siemens Healthcare, Forchheim, Germany), a 64-row CT scanner (Optima CT680, GE Healthcare, Milwaukee, WI, USA), a multidetector CT system (Discovery CT750 HD; GE Healthcare, USA), or a Brilliance CT Elite FHD scanner (Philips Healthcare, Best, The Netherlands). Scan parameters used on each system are shown in *Table 1*.

ICA was obtained using either an Axiom Artis angiography system (Siemens Healthcare, Erlangen, Germany), an Allura Xper FD20 angiography system (Philips Medical Systems, Best, the Netherlands), or an INNOVA 3100 digital plate angiography system (GE Healthcare, Waukesha, WI, USA). The contrast medium was injected manually, and the dosage was 20–30 mL.

Image analysis

In the CCTA-AI part of this study, CCTA images were automatically analyzed using a commercially available CCTA-AI platform package (Coronary Doc, ShuKun Technology, Beijing, China) without any human subjective intervention. This platform can automatically identify vascular segments and detect stenosis using maximum intensity projection, multiplanar reconstruction, curvature plane reconstruction, and volume reconstruction based on a CNN model (18).

In the CCTA reader part of this study, the CCTA images were evaluated by 2 cardiovascular radiologists (with 5–10 years of experience) independently on a post-processing workstation (Syngo Via, Siemens Healthineers, Forchheim, Germany). The radiologists were blinded to

Table 1 The scan parameters of different CT scanners in CCTA

Scan parameters	Siemens dual-source CT flash	GE Optima CT680	GE Discovery CT750 HD	PHILIPS Brilliance iCT Elite FHD
Tube voltage (kV)	80–100	100–120	100–120	100–120
Tube current (mAs)	Auto	Auto	Auto	Auto
Slice thickness (mm)	0.750	0.625	0.625	0.900
Slice gap (mm)	0.750	0.625	0.625	0.450
Field of view (cm)	150–200	150–200	150–200	150–200
Retrospective gating	Both	Both	Both	Both
Scan trigger mode	Bolus tracking	Test bolus	Test bolus	Bolus tracking
Contrast material volume (mL)	50–55	65–75	65–75	50–55
Contrast flow rate (g/s)	5.5–6.0	4.5–5.5	4.5–5.5	4.5–5.5
Contrast concentration (mgI/mL)	350–370	350–370	350–370	350–370

CCTA, coronary computed tomographic angiography.

each patient's outcome data. Disagreements were resolved by discussion until a consensus was reached.

ICA was performed with a standard position and image for each vessel according to standard procedures (21). All ICA images were re-evaluated visually by 1 experienced interventional cardiologist (Doctor A) who was blinded to the patient's CCTA images and clinical information. To ensure reliability, another interventional cardiologist (Doctor B) completed the assessment in a randomly selected group of 40 patients, and interclass correlation coefficients (ICCs) were used to evaluate the reproducibility. An ICC greater than 0.75 indicated good agreement of the data.

Each coronary artery was segmented according to the 18-segment model proposed by the Society of Cardiovascular Computed Tomography (SCCT) (22). After any coronary artery segment with a diameter of less than 2 mm was excluded, the proximal right coronary artery (pRCA), mid-right coronary artery (mRCA), distal right coronary artery (dRCA), right posterior descending artery (R-PDA), proximal left anterior descending artery (pLAD), mid-left anterior descending artery (mLAD), distal left anterior descending artery (dLAD), first diagonal branch (D1), proximal circumflex artery (pCx), first obtuse marginal artery (OM1), and left circumflex artery (LCx) remained. The cutoff values of models 1 and 2, were 50% and 70%, respectively. Model 1 compared stenosis rates between 0–49% and 50–100%. Model 2 compared stenosis rates between 1–69% and 70–100%.

Statistical analysis

Statistical analyses were performed using SPSS 21.0 (IBM Corp., Armonk, NY, USA), where statistical significance was considered at a level of $P<0.05$. Categorical variables were compared using the χ^2 test, whereas continuous variables were compared using the independent-sample *t* test or Mann–Whitney U test as appropriate following the Kolmogorov–Smirnov test of normality. Models 1 and 2 were used to determine the sensitivity (Se), specificity (Sp), positive predictive value (PPV), and negative predictive value (NPV) and their corresponding 95% confidence intervals (CIs). The diagnostic performances of AI for coronary artery stenosis with models 1 and 2 were evaluated using receiver operating characteristic (ROC) curves and quantitatively expressed using the area under the curve (AUC). ROC curve analysis was performed using MedCalc version 19.0 (MedCalc Platform bvba, Ostend, Belgium; https://www.medcalc.org; 2019).

Results

Patient characteristics

After applying strict inclusion and exclusion criteria, 318 patients with suspected chest pain were included in our final analysis (*Figure 1*). Among the numerous risk factors, hypertension (65%) was the most common, while incidence rates of other risk factors were less than 50%. The average

Table 2 Characteristics of the study participants

Characteristics	Value
Age (years), median ± standard deviation [range]	62±10 [29–86]
Male	223 [70]
Female	95 [30]
Hypertension	204 [65]
Hypercholesterolemia	74 [23]
Diabetes	123 [39]
Current smoking	122 [38]
Current drinking	78 [25]
Family history of CAD	25 [8]
Image quality (4-point Likert scale)	
3	127 [40]
4	191 [60]
The average post-processing time with CCTA-AI(s)[#]	20.4±4.1
The average post-processing time with the reader(s)[#]	1,112.1±122.8
ICA	
Lesion vessels	
None	12 [4]
One vessel	54 [17]
Two vessels	63 [20]
Three vessels	179 [56]
Four vessels	10 [3]
The degree of vascular stenosis at the patient level	
0%	13 [4]
1–24%	3 [1]
25–49%	29 [9]
50–69%	56 [18]
70–99%	160 [50]
100%	57 [18]

Unless otherwise indicated, data are numbers of patients, with percentages. [#], data are presented as the mean ± standard deviation. ICA, invasive coronary angiography; CAD, coronary artery disease; CCTA, coronary computed tomographic angiography; AI, artificial intelligence.

post-processing times of the CCTA-AI platform and CCTA reader were 20.4±4.1 and 1,112.1±122.8 s, respectively. The degree of vascular stenosis and the number of lesion vessels at the patient level of ICA are shown in *Table 2*. Other detailed demographic and clinical characteristics are shown in *Table 2*. The ICCs of 2 interventional cardiologists ranged from 0.806 to 0.100, indicating good interobserver assessment reproducibility.

Patient-level analysis

Table 3 describes the detailed data of no visible (0), minimal (1–24%), mild (25–49%), moderate (50–69%), severe stenosis (70–99%), and occluded (100%) of the segment level of vascular stenosis on CCTA-AI and CCTA reader. The specific diagnostic performance parameters of CCTA-AI assessed the detection of vessel stenosis at the patient level, as displayed in *Table 4*. The ROC results for these comparisons are illustrated in *Figure 2*. The AUCs (0.85 and 0.78) were obtained by the CCTA-AI platform using the bounds of models 1 and 2. The AUCs obtained by the CCTA reader were 0.61 and 0.64 for models 1 and 2, respectively. At the patient level, the AUC of CCTA-AI was significantly better than that of the CCTA reader.

Segment-level analysis

Coronary artery segments were analyzed based on SCCT. Coronary artery stenosis of CCTA and ICA were categorized by order of the stenosis grade. The segments of pRCA, mRCA, dRCA, LM, pLAD, mLAD, dLAD, D1, pCx, OM1, and LCx were included. The detailed diagnostic parameters of CCTA-AI and CCTA reader assessed using the segment-based analysis were compared as shown in *Tables 5-8*.

The diagnostic performance of the CCTA-AI platform and CCTA reader at the segment level was moderate for models 1 and 2 (see *Figure 3* for specific examples). Furthermore, the AUCs of CCTA-AI were slightly better than those of the CCTA reader in models 1 and 2. With the stenosis cutoff value increasing from model 1 to 2, the diagnostic values of Sp and NPV showed a gradually increasing trend. Conversely, the Se showed a gradually decreasing trend. Meanwhile, the diagnostic performances

Table 3 Description of the segment level of vascular stenosis by the CCTA-AI platform and the CCTA reader

Vessels stenosis	pRCA	mRCA	dRCA	LM	pLAD	mLAD	dLAD	D1	pCx	OM1	LCx
CCTA-AI, n [%]											
0	111 [35]	139 [44]	182 [57]	201 [63]	114 [36]	93 [29]	288 [90]	241 [75]	166 [52]	272 [85]	197 [62]
1–24%	26 [8]	21 [6]	18 [6]	42 [13]	36 [11]	14 [4]	8 [3]	28 [9]	29 [9]	12 [4]	27 [9]
25–49%	85 [27]	80 [25]	56 [18]	49 [15]	73 [23]	75 [24]	14 [4]	21 [7]	73 [23]	17 [5]	44 [14]
50–69%	64 [20]	50 [16]	48 [15]	20 [6]	66 [21]	91 [29]	7 [2]	18 [6]	33 [11]	14 [4]	30 [9]
70–99%	27 [8]	26 [8]	14 [4]	6 [2]	27 [8]	44 [14]	1 [1]	10 [3]	17 [5]	2 [1]	20 [6]
100%	5 [2]	2 [1]	0 [0]	0 [0]	2 [1]	1 [0]	0 [0]	0 [0]	0 [0]	1 [1]	0 [0]
CCTA reader, n [%]											
0	126 [39]	153 [48]	209 [66]	223 [70]	60 [19]	120 [38]	285 [89]	256 [80]	153 [48]	284 [89]	211 [66]
1–24%	34 [11]	28 [9]	13 [4]	57 [18]	26 [8]	15 [5]	3 [1]	16 [5]	47 [15]	8 [3]	15 [5]
25–49%	72 [23]	55 [17]	46 [14]	29 [9]	79 [25]	45 [14]	15 [5]	21 [7]	48 [15]	12 [4]	21 [7]
50–69%	26 [8]	42 [13]	21 [7]	7 [2]	56 [17]	59 [18]	8 [3]	15 [5]	26 [8]	8 [3]	27 [8]
70–99%	59 [18]	40 [13]	29 [9]	2 [1]	97 [31]	79 [25]	7 [2]	10 [3]	43 [13]	6 [2]	39 [12]
100%	1 [1]	0 [0]	0 [0]	0 [0]	0 [0]	0 [0]	0 [0]	0 [0]	1 [1]	0 [0]	5 [2]

CCTA, coronary computed tomographic angiography; AI, artificial intelligence; pRCA, proximal right coronary artery; mRCA, mid-right coronary artery; dRCA, distal right coronary artery; pLAD, proximal left anterior descending artery; mLAD, mid-left anterior descending artery; dLAD, distal left anterior descending artery; D1, first diagonal branch; pCx, proximal circumflex artery; OM1, first obtuse marginal artery; LCx, left circumflex artery.

Table 4 The diagnostic performances of the CCTA-AI platform and reader on patient-based analyses

Accuracy parameters	The diagnostic efficacy in model 1		The diagnostic efficacy in model 2	
	CCTA-AI	Reader	CCTA-AI	Reader
TP	245	192	109	135
FP	13	80	13	78
FN	28	16	108	25
TN	32	30	88	80
Se, % [95% CI]	90 [85–93]	93 [88–95]	50 [43–57]	84 [78–89]
Sp, % [95% CI]	71 [55–83]	27 [19–37]	87 [79–93]	51 [43–59]
PPV, % [95% CI]	95 [91–97]	71 [65–76]	89 [82–94]	63 [56–70]
NPV, % [95% CI]	53 [40–66]	65 [50–78]	45 [38–52]	76 [67–84]
AUC, % [95% CI]	85 [81–89]	61 [56–67]	78 [73–82]	64 [58–69]

Numbers in parentheses are 95% CIs. CCTA, coronary computed tomographic angiography; AI, artificial intelligence; TP, true positive; FP, false positive; FN, false negative; TN, true negative; Se, sensitivity; Sp, specificity; PPV, positive predictive value; NPV, negative predictive value; AUC, the area under the curve; CI, confidence interval.

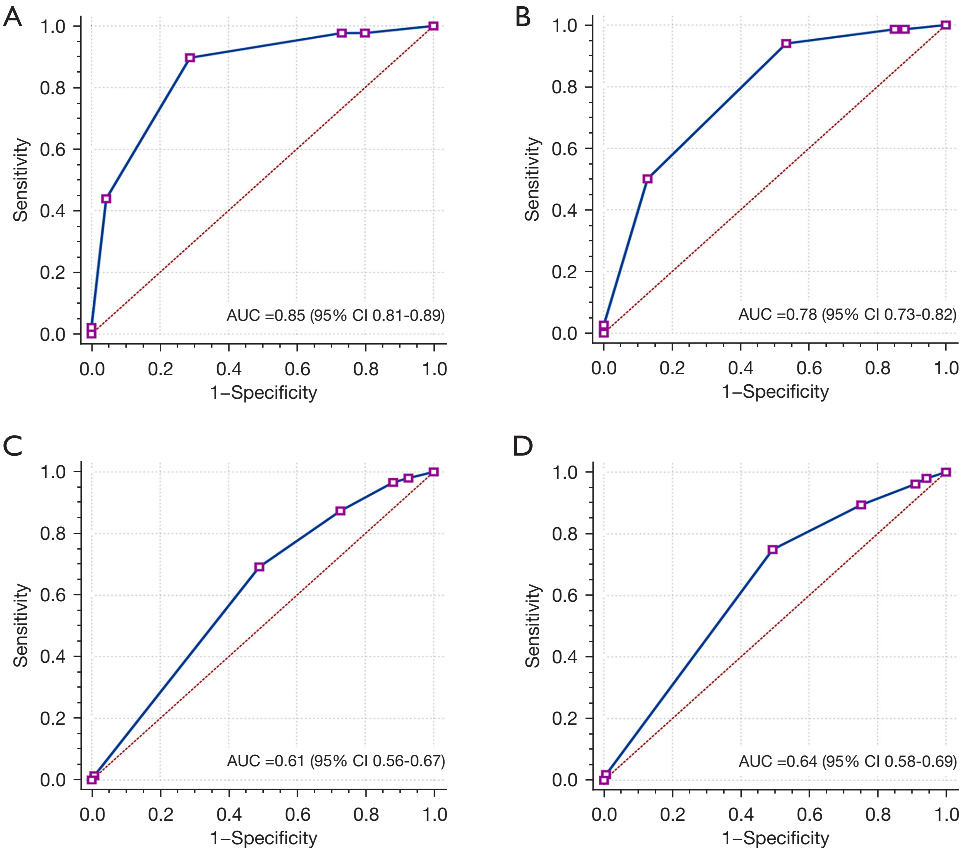

Figure 2 The graph shows the performance of the CCTA-AI platform and the CCTA reader for models 1 and 2 in the patient-based analysis. (A) The CCTA-AI platform showed an AUC of 0.85 in the classification of model 1. (B) The CCTA-AI platform showed an AUC of 0.78 in the classification of model 2. (C) The CCTA reader showed an AUC of 0.61 in the classification of model 1. (D) The CCTA reader showed an AUC of 0.64 in the classification of model 2. CCTA, coronary computed tomographic angiography; AI, artificial intelligence; AUC, the area under the curve; CI, confidence interval.

for segments of large-diameter vessels were better than for narrower ones. For instance, the AUCs of CCTA-AI for identifying stenosis in the pRCA, mRCA, and dRCA segments using model 1 were 0.73, 0.70, and 0.69, respectively.

Discussion

This study aimed to explore the diagnostic performance of one commercialized CCTA-AI platform for the evaluation of coronary artery stenosis compared with a CCTA reader using external multicenter and multidevice data. The main findings of the study can be summarized as follows: (I) at the patient level, the CCTA-AI platform provided a useful tool for the diagnosis of coronary artery stenosis, with significantly improved diagnostic efficiency; and (II) at the segment level, the CCTA-AI platform with models 1 and 2 exhibited moderate diagnostic performance that was slightly better than that of the CCTA reader. In addition, the diagnostic performance in narrow-diameter segments was comparatively weaker.

The results demonstrated that the CCTA-AI platform had a relatively moderate diagnostic performance in the diagnosis of coronary stenosis. The platform was able to accurately identify coronary artery stenosis at the patient level, with results consistent with those of other similar studies (23,24). Thus, the CCTA-AI platform has the potential to be a reliable diagnostic tool for the detection of coronary artery stenosis. In addition, compared with manual processing and reporting times ranging from 18 to 85 minutes, as reported in our and other previous studies (25,26), the mean automatic post-processing time of the

Table 5 The diagnostic parameters of the reader on segment-based analyses for model 1

Accuracy parameters	pRCA	mRCA	dRCA	LM	pLAD	mLAD	dLAD	D1	pCx	OM1	LCx
N	318	318	318	318	318	318	318	318	318	318	318
Prevalence of stenosis, n [%]	87 [27]	81 [25]	38 [12]	15 [5]	144 [45]	121 [38]	23 [7]	49 [15]	70 [22]	28 [9]	61 [19]
TP	43	37	17	6	90	65	2	9	34	6	45
FP	44	45	33	3	63	73	13	16	40	8	26
FN	43	44	21	9	54	56	21	40	40	22	50
TN	188	192	247	300	111	124	282	253	208	282	197
Se, % [95% CI]	50 [39–61]	46 [35–57]	45 [29–62]	40 [17–67]	63 [54–70]	54 [44–63]	9 [1–30]	18 [9–33]	46 [34–58]	21 [9–41]	47 [37–58]
Sp, % [95% CI]	81 [75–86]	81 [75–86]	88 [84–92]	99 [97–100]	64 [56–71]	63 [56–70]	96 [92–98]	94 [90–96]	84 [79–88]	97 [94–99]	88 [83–92]
PPV, % [95% CI]	49 [39–60]	45 [34–56]	34 [22–49]	67 [31–91]	59 [51–67]	47 [39–56]	13 [2–42]	36 [19–57]	46 [34–58]	43 [19–70]	63 [51–74]
NPV, % [95% CI]	81 [76–86]	81 [76–86]	92 [88–95]	97 [94–99]	67 [59–74]	69 [62–75]	93 [89–96]	86 [82–90]	84 [79–88]	93 [89–95]	80 [74–84]
AUC, % [95% CI]	66 [60–71]	63 [58–69]	67 [61–72]	70 [64–75]	63 [58–69]	58 [53–64]	52 [47–58]	56 [51–62]	65 [60–71]	59 [54–65]	68 [62–73]

TP, true positive; FP, false positive; FN, false negative; TN, true negative; Se, sensitivity; Sp, specificity; PPV, positive predictive value; NPV, negative predictive value; AUC, the area under the curve; CI, confidence interval; pRCA, proximal right coronary artery; mRCA, mid-right coronary artery; dRCA, distal right coronary artery; pLAD, proximal left anterior descending artery; mLAD, mid-left anterior descending artery; dLAD, distal left anterior descending artery; D1, first diagonal branch; pCx, proximal circumflex artery; OM1, first obtuse marginal artery; LCx, left circumflex artery.

Table 6 The diagnostic parameters of the CCTA-AI platform on segment-based analyses for model 1

Accuracy parameters	pRCA	mRCA	dRCA	LM	pLAD	mLAD	dLAD	D1	pCx	OM1	LCx
N	318	318	318	318	318	318	318	318	318	318	318
Prevalence of stenosis, n [%]	86 [27]	77 [24]	34 [11]	13 [4]	137 [43]	114 [36]	21 [7]	48 [15]	66 [21]	28 [9]	93 [29]
TP	42	38	15	8	65	71	2	8	23	5	30
FP	44	42	45	14	33	67	5	13	14	9	18
FN	41	39	19	5	72	43	19	40	43	23	63
TN	191	199	239	291	148	137	293	257	238	281	207
Se, % [95% CI]	51 [39–62]	49 [38–61]	44 [28–62]	62 [32–85]	47 [39–56]	62 [53–71]	9 [1–32]	17 [8–31]	35 [24–48]	18 [7–38]	32 [23–43]
Sp, % [95% CI]	81 [76–86]	83 [77–87]	84 [79–88]	95 [92–97]	82 [75–87]	67 [60–73]	98 [96–99]	95 [92–97]	94 [91–97]	97 [94–98]	92 [87–95]
PPV, % [95% CI]	49 [38–60]	48 [36–59]	25 [15–38]	36 [18–59]	66 [56–75]	51 [43–60]	29 [5–70]	38 [19–61]	62 [45–77]	36 [14–64]	63 [47–76]
NPV, % [95% CI]	82 [77–87]	84 [78–88]	93 [89–95]	98 [96–99]	67 [61–73]	76 [69–82]	94 [90–96]	87 [82–90]	85 [80–86]	92 [89–95]	77 [71–81]
AUC, % [95% CI]	73 [68–78]	70 [64–75]	67 [61–72]	79 [74–84]	70 [65–75]	67 [61–72]	53 [47–59]	64 [58–69]	73 [68–78]	62 [57–68]	69 [63–74]

CCTA, coronary computed tomographic angiography; AI, artificial intelligence; TP, true positive; FP, false positive; FN, false negative; TN, true negative; Se, sensitivity; Sp, specificity; PPV, positive predictive value; NPV, negative predictive value; AUC, the area under the curve; CI, confidence interval; pRCA, proximal right coronary artery; mRCA, mid-right coronary artery; dRCA, distal right coronary artery; pLAD, proximal left anterior descending artery; mLAD, mid-left anterior descending artery; dLAD, distal left anterior descending artery; D1, first diagonal branch; pCx, proximal circumflex artery; OM1, first obtuse marginal artery; LCx, left circumflex artery.

Table 7 The diagnostic parameters of the reader on segment-based analyses for model 2

Accuracy parameters	pRCA	mRCA	dRCA	LM	pLAD	mLAD	dLAD	D1	pCx	OM1	LCx
Number	318	318	318	318	318	318	318	318	318	318	318
Prevalence of stenosis, n [%]	51 [16]	48 [15]	24 [8]	8 [3]	103 [32]	78 [25]	14 [4]	30 [9]	47 [15]	20 [6]	61 [19]
TP	27	16	8	1	54	32	1	5	19	4	24
FP	24	24	21	1	43	47	13	5	25	2	20
FN	24	32	16	7	49	46	21	25	28	16	37
TN	233	246	273	309	172	193	282	283	246	296	237
Se, % [95% CI]	53 (39–67)	33 (21–49)	33 (16–55)	13 (1–53)	52 (42–62)	41 (30–53)	7 (0–36)	17 (6–25)	40 (27–56)	20 (7–44)	39 (27–53)
Sp, % [95% CI]	91 (86–94)	91 (87–94)	93 (89–95)	100 (98–100)	80 (74–85)	80 (75–85)	98 (96–99)	98 (96–99)	91 (87–94)	99 (97–100)	92 (88–95)
PPV, % [95% CI]	53 (39–67)	40 (25–57)	28 (13–47)	50 (3–97)	56 (45–66)	41 (30–52)	14 (1–58)	50 (20–80)	43 (29–59)	67 (24–94)	55 (39–63)
NPV, % [95% CI]	91 (86–94)	88 (84–92)	94 (91–97)	98 (95–99)	78 (72–83)	81 (75–85)	96 (93–98)	92 (88–95)	90 (85–93)	95 (92–97)	86 (82–90)
AUC, % [95% CI]	70 (65–75)	62 (57–68)	63 (58–68)	56 (50–62)	66 (61–71)	61 (55–66)	53 (47–58)	58 (52–63)	66 (60–71)	60 (54–65)	66 (60–71)

TP, true positive; FP, false positive; FN, false negative; TN, true negative; Se, sensitivity; Sp, specificity; PPV, positive predictive value; NPV, negative predictive value; AUC, the area under the curve; CI, confidence interval; pRCA, proximal right coronary artery; mRCA, mid-right coronary artery; dRCA, distal right coronary artery; pLAD, proximal left anterior descending artery; mLAD, mid-left anterior descending artery; dLAD, distal left anterior descending artery; D1, first diagonal branch; pCx, proximal circumflex artery; OM1, first obtuse marginal artery; LCx, left circumflex artery.

Table 8 The diagnostic parameters of the CCTA-AI platform on segment-based analysis for model 2

Accuracy parameters	pRCA	mRCA	dRCA	LM	pLAD	mLAD	dLAD	D1	pCx	OM1	LCx
No	318	318	318	318	318	318	318	318	318	318	318
Prevalence of stenosis, n [%]	50 [16]	77 [24]	34 [11]	6 [2]	98 [31]	72 [23]	12 [4]	52 [16]	40 [13]	20 [6]	60 [19]
TP	12	8	3	3	20	19	0	4	5	0	13
FP	12	14	11	1	8	24	1	2	2	1	7
FN	38	37	17	3	78	53	12	25	35	20	47
TN	256	259	287	311	212	222	305	287	276	297	251
Se, % [95% CI]	24 (14–38)	18 (9–33)	15 (4–39)	50 (14–86)	20 (13–30)	26 (17–38)	0 (0–30)	14 (5–33)	13 (5–28)	0 (0–20)	22 (12–35)
Sp, % [95% CI]	96 (92–98)	95 (91–97)	96 (93–98)	100 (98–100)	96 (93–98)	90 (86–94)	100 (98–100)	99 (97–100)	99 (97–100)	100 (98–100)	97 (94–99)
PPV, % [95% CI]	50 (30–70)	36 (18–59)	21 (6–51)	75 (22–99)	71 (51–86)	44 (29–60)	0 (0–95)	67 (24–94)	71 (30–95)	0 (0–95)	65 (41–84)
NPV, % [95% CI]	87 (83–91)	88 (83–91)	94 (91–97)	99 (97–100)	73 (68–78)	81 (75–85)	96 (93–98)	92 (88–95)	89 (85–92)	94 (90–96)	84 (79–88)
AUC, % [95% CI]	75 (70–80)	74 (68–78)	69 (64–74)	88 (83–91)	70 (65–75)	65 (60–70)	58 (53–64)	66 (60–71)	70 (65–75)	64 (59–70)	69 (64–74)

CCTA, coronary computed tomographic angiography; AI, artificial intelligence; TP, true positive; FP, false positive; FN, false negative; TN, true negative; Se, sensitivity; Sp, specificity; PPV, positive predictive value; NPV, negative predictive value; AUC, the area under the curve; CI, confidence interval; pRCA, proximal right coronary artery; mRCA, mid-right coronary artery; dRCA, distal right coronary artery; pLAD, proximal left anterior descending artery; mLAD, mid-left anterior descending artery; dLAD, distal left anterior descending artery; D1, first diagonal branch; pCx, proximal circumflex artery; OM1, first obtuse marginal artery; LCx, left circumflex artery.

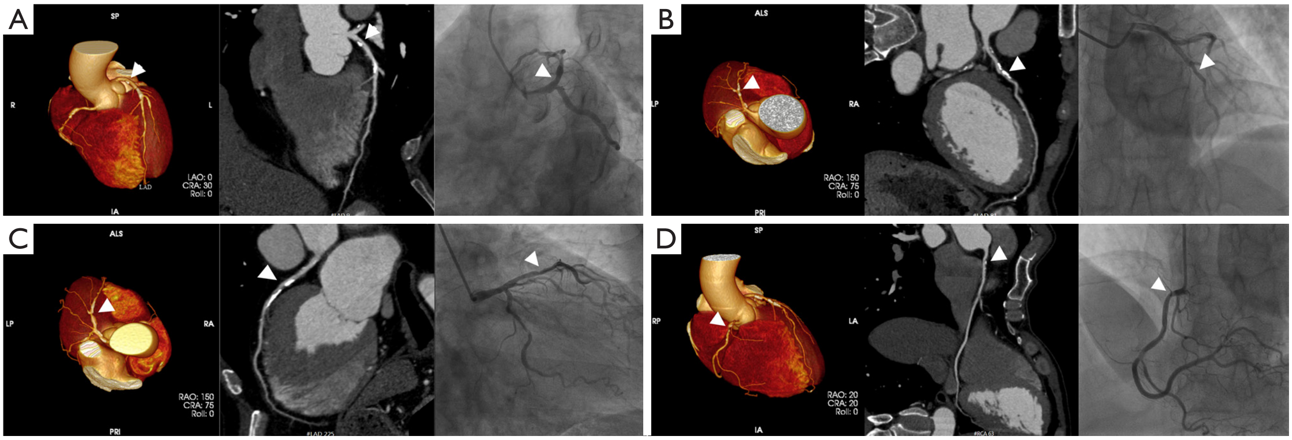

Figure 3 The specific cases were reported based on CCTA-AI, CCTA reader and ICA. (A) A 54-year-old male. At the proximal left anterior descending artery (pLAD), the diagnosis of CCTA-AI, CCTA reader, and ICA are mild stenoses (25% to 49%). (B) A 56-year-old male. At the proximal left anterior descending artery (pLAD), the diagnosis of CCTA-AI and CCTA reader are moderate stenoses (50% to 69%), while the ICA is mild stenosis. (C) A 62-year-old male. At the proximal left anterior descending artery (pLAD), the diagnosis of CCTA-AI and CCTA reader are mild stenoses, while the ICA is severe stenosis (70% to 99%). (D) A 57-year-old female. At the proximal right coronary artery (pRCA), the diagnosis of CCTA-AI is minimal stenosis (1% to 24%), then CCTA reader is mild stenosis, while the ICA is minimal stenosis. Lesions are marked with white arrows. CCTA, coronary computed tomographic angiography; AI, artificial intelligence; ICA, invasive coronary angiography.

CCTA-AI platform was 20.4 seconds. As such, this platform could significantly reduce the work burden of doctors while improving diagnostic efficiency.

The diagnostic performance of CCTA-AI depends on the degree of stenosis at the segment level. At the segment level, compared with model 1, the diagnostic Se of model 2 was generally lower. In contrast, the diagnostic Sp, NPV, and AUC increased. This finding may be related to CCTA itself estimating a relatively high NPV in the judgment of vessel stenosis, particularly in cases of severely stenotic vessels (27). Another factor may be that more severe stenoses tend to exhibit more severe vascular calcification. Consequently, the quantification of stenosis can be overestimated due to artifacts caused by coronary calcification (28). These findings are consistent with those of previous CCTA studies (7,29).

The diagnostic efficacy at the segment level was closely related to the vessel diameter. The Se, PPV, and AUC of large-diameter vessels were comparatively higher than those of narrower ones. Conversely, the Sp and NPV showed the opposite trend. This finding may be due to the impact of CT artifacts in images of narrow vessels caused by cardiac arrhythmia, dense calcifications, or other artifact sources (30). Alternatively, it may be that CCTA has an intrinsically lower accuracy for narrower vessels (especially those <2 mm), as reported previously (29). Thus far, the vast majority of research in this area has focused on diagnostic capacity in the major branches of the coronary artery (31). In summary, the diagnostic performance of narrow-vessel stenosis by CCTA-AI may be relatively limited, which might be down to the nature of CCTA itself, but more external data validation is required to confirm it.

In this study, the CCTA-AI platform was based on a CNN model. CNN models have been widely used for object detection, classification, and segmentation, including in medical images (32-34). Similarly, in cardiovascular research, CNN models have been used to overcome some important issues. Some limitations of these models have been reported, specifically that CCTA-AI has been shown to have limited performance in the diagnosis of narrow vessels (35). Therefore, it might be necessary to introduce CCTA-AI correction measures to correct or compensate for this systematic deviation. It is important to note that the correction must follow a certain rule, for example, coronary artery disease-reporting and data system (CAD-RADS) or CCTA-AI results. However, this is only a preliminary suggestion, and further large-scale multicenter studies using AI computational modeling are needed to confirm the appropriateness of this course of action.

There were some limitations to this study. Although this was a multicenter and multidevice study involving a relatively large sample, the extent and the distribution of disease severity were relatively small and non-homogeneous. More varied data are required to provide a robust AI model. Second, the study did not assess the nature of the plaque or the CT-FFR when evaluating the prognoses of patients and coronary artery hemodynamic effects, even though these are both crucial pieces of information in the treatment of CAD.

Conclusions

This study shows that the commercial CCTA-AI platform may provide a feasible and useful tool for diagnosing coronary artery stenosis at the patient level, as shown using an external multicenter and multidevice dataset. This technology could significantly improve the diagnostic efficiency of stenosis, and radiologists could use the technology as a one-stop tool for rapid post-processing of images. However, the ability of this technology to be used to make a diagnosis, particularly for smaller branches or distal vessels, still needs to be improved.

Acknowledgments

Funding: This work was supported in part by the Chongqing City Science, Technology, and Health Joint Project (No. 2021msxm341) and in part by the Chongqing City Technology Innovation and Application Development (No. cstc2019jscx-msxmX0126).

Footnote

Reporting Checklist: The authors have completed the STARD reporting checklist. Available at https://qims.amegroups.com/article/view/10.21037/qims-22-1115/rc

Conflicts of Interest: All authors have completed the ICMJE uniform disclosure form (available at https://qims.amegroups.com/article/view/10.21037/qims-22-1115/coif). The authors have no conflicts of interest to declare.

Ethical Statement: The authors are accountable for all aspects of the work in ensuring that questions related to the accuracy or integrity of any part of the work are appropriately investigated and resolved. The study was conducted in accordance with the Declaration of Helsinki (as revised in 2013). This study was approved by Southwest Hospital, Third Military Medical University [Army Medical University (No. KY2020306)] and the medical science research ethics committees of 3 other hospitals [The Second People's Hospital of Liao Cheng (No. 2021-8); UIanqab Central Hospital (No. 2021-3); LinFen central hospital (No. 2021-23-1)]. The requirement for individual consent for this retrospective analysis was waived.

References

1. Zhou M, Wang H, Zeng X, Yin P, Zhu J, Chen W, et al. Mortality, morbidity, and risk factors in China and its provinces, 1990-2017: a systematic analysis for the Global Burden of Disease Study 2017. Lancet 2019;394:1145-58.
2. Benjamin EJ, Muntner P, Alonso A, Bittencourt MS, Callaway CW, Carson AP, et al. Heart Disease and Stroke Statistics-2019 Update: A Report From the American Heart Association. Circulation 2019;139:e56-e528.
3. Head SJ, Milojevic M, Daemen J, Ahn JM, Boersma E, Christiansen EH, et al. Mortality after coronary artery bypass grafting versus percutaneous coronary intervention with stenting for coronary artery disease: a pooled analysis of individual patient data. Lancet 2018;391:939-48.
4. Bartorelli AL, Andreini D, Mushtaq S, Serruys PW. The revolution project: replacing coronary artery angiography with coronary computed tomography with functional evaluation. Eur Heart J Suppl 2020;22:L15-8.
5. Gulati M, Levy PD, Mukherjee D, Amsterdam E, Bhatt DL, Birtcher KK, et al. 2021 AHA/ACC/ASE/CHEST/SAEM/SCCT/SCMR Guideline for the Evaluation and Diagnosis of Chest Pain: Executive Summary: A Report of the American College of Cardiology/American Heart Association Joint Committee on Clinical Practice Guidelines. Circulation 2021;144:e368-454.
6. Hoffmann U, Truong QA, Schoenfeld DA, Chou ET, Woodard PK, Nagurney JT, et al. Coronary CT angiography versus standard evaluation in acute chest pain. N Engl J Med 2012;367:299-308.
7. Knuuti J, Wijns W, Saraste A, Capodanno D, Barbato E, Funck-Brentano C, et al. 2019 ESC Guidelines for the

diagnosis and management of chronic coronary syndromes. Eur Heart J 2020;41:407-77.
8. Nicol ED, Norgaard BL, Blanke P, Ahmadi A, Weir-McCall J, Horvat PM, Han K, Bax JJ, Leipsic J. The Future of Cardiovascular Computed Tomography: Advanced Analytics and Clinical Insights. JACC Cardiovasc Imaging 2019;12:1058-72.
9. Kang D, Dey D, Slomka PJ, Arsanjani R, Nakazato R, Ko H, Berman DS, Li D, Kuo CC. Structured learning algorithm for detection of nonobstructive and obstructive coronary plaque lesions from computed tomography angiography. J Med Imaging (Bellingham) 2015;2:014003.
10. He J, Baxter SL, Xu J, Xu J, Zhou X, Zhang K. The practical implementation of artificial intelligence technologies in medicine. Nat Med 2019;25:30-6.
11. Retson TA, Besser AH, Sall S, Golden D, Hsiao A. Machine Learning and Deep Neural Networks in Thoracic and Cardiovascular Imaging. J Thorac Imaging 2019;34:192-201.
12. Krittanawong C, Johnson KW, Rosenson RS, Wang Z, Aydar M, Baber U, Min JK, Tang WHW, Halperin JL, Narayan SM. Deep learning for cardiovascular medicine: a practical primer. Eur Heart J 2019;40:2058-73.
13. Rønnow Sand NP, Nissen L, Winther S, Petersen SE, Westra J, Christiansen EH, Larsen P, Holm NR, Isaksen C, Urbonaviciene G, Deibjerg L, Husain M, Thomsen KK, Rohold A, Bøtker HE, Bøttcher M. Prediction of Coronary Revascularization in Stable Angina: Comparison of FFR(CT) With CMR Stress Perfusion Imaging. JACC Cardiovasc Imaging 2020;13:994-1004.
14. Wan KW, Wong CH, Ip HF, Fan D, Yuen PL, Fong HY, Ying M. Evaluation of the performance of traditional machine learning algorithms, convolutional neural network and AutoML Vision in ultrasound breast lesions classification: a comparative study. Quant Imaging Med Surg 2021;11:1381-93.
15. Al'Aref SJ, Anchouche K, Singh G, Slomka PJ, Kolli KK, Kumar A, et al. Clinical applications of machine learning in cardiovascular disease and its relevance to cardiac imaging. Eur Heart J 2019;40:1975-86.
16. Betancur J, Commandeur F, Motlagh M, Sharir T, Einstein AJ, Bokhari S, Fish MB, Ruddy TD, Kaufmann P, Sinusas AJ, Miller EJ, Bateman TM, Dorbala S, Di Carli M, Germano G, Otaki Y, Tamarappoo BK, Dey D, Berman DS, Slomka PJ. Deep Learning for Prediction of Obstructive Disease From Fast Myocardial Perfusion SPECT: A Multicenter Study. JACC Cardiovasc Imaging 2018;11:1654-63.
17. Zreik M, Lessmann N, van Hamersvelt RW, Wolterink JM, Voskuil M, Viergever MA, Leiner T, Išgum I. Deep learning analysis of the myocardium in coronary CT angiography for identification of patients with functionally significant coronary artery stenosis. Med Image Anal 2018;44:72-85.
18. Han D, Liu J, Sun Z, Cui Y, He Y, Yang Z. Deep learning analysis in coronary computed tomographic angiography imaging for the assessment of patients with coronary artery stenosis. Comput Methods Programs Biomed 2020;196:105651.
19. Li Y, Qiu H, Hou Z, Zheng J, Li J, Yin Y, Gao R. Additional value of deep learning computed tomographic angiography-based fractional flow reserve in detecting coronary stenosis and predicting outcomes. Acta Radiol 2022;63:133-40.
20. Dai X, Yu M, Pan J, Lu Z, Shen C, Wang Y, Lu B, Zhang J. Image quality and diagnostic accuracy of coronary CT angiography derived from low-dose dynamic CT myocardial perfusion: a feasibility study with comparison to invasive coronary angiography. Eur Radiol 2019;29:4349-56.
21. Dai S, Ding M, Liang N, Li Z, Li D, Guan L, Liu H. Associations of ACE I/D polymorphism with the levels of ACE, kallikrein, angiotensin II and interleukin-6 in STEMI patients. Sci Rep 2019;9:19719.
22. Leipsic J, Abbara S, Achenbach S, Cury R, Earls JP, Mancini GJ, Nieman K, Pontone G, Raff GL. SCCT guidelines for the interpretation and reporting of coronary CT angiography: a report of the Society of Cardiovascular Computed Tomography Guidelines Committee. J Cardiovasc Comput Tomogr 2014;8:342-58.
23. Chen M, Wang X, Hao G, Cheng X, Ma C, Guo N, Hu S, Tao Q, Yao F, Hu C. Diagnostic performance of deep learning-based vascular extraction and stenosis detection technique for coronary artery disease. Br J Radiol 2020;93:20191028.
24. Zreik M, van Hamersvelt RW, Wolterink JM, Leiner T, Viergever MA, Isgum I. A Recurrent CNN for Automatic Detection and Classification of Coronary Artery Plaque and Stenosis in Coronary CT Angiography. IEEE Trans Med Imaging 2019;38:1588-98.
25. Liu K, Hsieh C, Zhuang N, Gao Y, Li Z, Ren X, Yang L, Zhang J, Budoff MJ, Lu B. Current utilization of cardiac computed tomography in mainland China: A national survey. J Cardiovasc Comput Tomogr 2016;10:76-81.
26. Benjamin MM, Rabbat MG. Machine learning-based advances in coronary computed tomography angiography. Quant Imaging Med Surg 2021;11:2208-13.
27. Williams MC, Moss A, Nicol E, Newby DE. Cardiac CT

Improves Outcomes in Stable Coronary Heart Disease: Results of Recent Clinical Trials. Curr Cardiovasc Imaging Rep 2017;10:14.

28. Murgia A, Balestrieri A, Crivelli P, Suri JS, Conti M, Cademartiri F, Saba L. Cardiac computed tomography radiomics: an emerging tool for the non-invasive assessment of coronary atherosclerosis. Cardiovasc Diagn Ther 2020;10:2005-17.
29. Miller JM, Rochitte CE, Dewey M, Arbab-Zadeh A, Niinuma H, Gottlieb I, Paul N, Clouse ME, Shapiro EP, Hoe J, Lardo AC, Bush DE, de Roos A, Cox C, Brinker J, Lima JA. Diagnostic performance of coronary angiography by 64-row CT. N Engl J Med 2008;359:2324-36.
30. Abdelrahman KM, Chen MY, Dey AK, Virmani R, Finn AV, Khamis RY, Choi AD, Min JK, Williams MC, Buckler AJ, Taylor CA, Rogers C, Samady H, Antoniades C, Shaw LJ, Budoff MJ, Hoffmann U, Blankstein R, Narula J, Mehta NN. Coronary Computed Tomography Angiography From Clinical Uses to Emerging Technologies: JACC State-of-the-Art Review. J Am Coll Cardiol 2020;76:1226-43.
31. Yoneyama H, Nakajima K, Taki J, Wakabayashi H, Matsuo S, Konishi T, Okuda K, Shibutani T, Onoguchi M, Kinuya S. Ability of artificial intelligence to diagnose coronary artery stenosis using hybrid images of coronary computed tomography angiography and myocardial perfusion SPECT. Eur J Hybrid Imaging 2019;3:4.
32. McKinney SM, Sieniek M, Godbole V, Godwin J, Antropova N, Ashrafian H, et al. International evaluation of an AI system for breast cancer screening. Nature 2020;577:89-94.
33. Zech JR, Badgeley MA, Liu M, Costa AB, Titano JJ, Oermann EK. Variable generalization performance of a deep learning model to detect pneumonia in chest radiographs: A cross-sectional study. PLoS Med 2018;15:e1002683.
34. Greenspan H, van Ginneken B, Summers RM. Guest Editorial Deep Learning in Medical Imaging: Overview and Future Promise of an Exciting New Technique. IEEE Transactions on Medical Imaging 2016;35:1153-9.
35. Muscogiuri G, Van Assen M, Tesche C, De Cecco CN, Chiesa M, Scafuri S, Guglielmo M, Baggiano A, Fusini L, Guaricci AI, Rabbat MG, Pontone G. Artificial Intelligence in Coronary Computed Tomography Angiography: From Anatomy to Prognosis. Biomed Res Int 2020;2020:6649410.

Cite this article as: Han Q, Jing F, Sun Z, Liu F, Zhang J, Wang J, Liang H. Validation of the commercial coronary computed tomographic angiography artificial intelligence for coronary artery stenosis: a cross-sectional study. Quant Imaging Med Surg 2023;13(6):3789-3801. doi: 10.21037/qims-22-1115

